Journal of Structural Geology, Vol. 15, Nos 3–5, pp. 309 to 322, 1993
Printed in Great Britain

0191-8141/93 $06.00 + 0.00

The structural anatomy of the Sandur schist belt—a greenstone belt in the Dharwar craton of South India

DHRUBA MUKHOPADHYAY

Department of Geology, University of Calcutta, 35 Ballygunge Circular Road, Calcutta 700019, India

and

ABDUL MATIN

Department of Geology, Ashutosh College, Calcutta 700026, India

(*Received* 3 *January* 1992; *accepted in revised form* 18 *September* 1992)

Abstract—Two belts of metasedimentary rocks occurring at the eastern and western flanks and a central terrane of metavolcanic rocks make up the Late Archaean Sandur schist belt in the Dharwar craton of South India. Contrary to the traditional interpretations, the regional structure of the belt is not a synclinorium.

The earliest episode of deformation produced major and minor isoclinal folds in the banded iron formation (BIF); their axial planes are parallel to the regional attitude of bedding. D_2 folds have a consistent sinistral sense of vergence throughout the schist belt and they refold the D_1 folds. The D_2 axial planes make small angles with regional bedding. There was a strong component of layer-parallel simple shear during D_2 deformation. The styles of D_1 and D_2 folds show a general similarity. The fold axes have variable plunge, though in general it is moderate to steep. The variability of the geometry of minor folds is ascribed to progressive development of folds and the rotation of their axes and axial planes during non-coaxial deformation (simple shear). It is likely that the D_1 and D_2 structures were not products of entirely unrelated episodes of deformation and they might have formed at the early and late stages of a progressive deformation history. A noteworthy feature is that the deformation is mostly concentrated in the two metasedimentary belts and the internal strain is low in the central metavolcanic unit. This is probably due to concentration of layer-parallel simple shear in the metasedimentary rocks.

Both flattening and simple shear played major roles in the development of the structural pattern and the deformation regime may be compared to one of transpression.

INTRODUCTION

THE Sandur schist belt is one of the Precambrian supracrustal belts, collectively known as the Dharwar schist belts, in the Dharwar craton of South India (Fig. 1). The rocks of the Dharwar Supergroup constituting these schist belts were laid down on the basement of 3.4–3.0 Ga old Peninsular Gneiss Complex (Swaminath *et al.* 1976). During the present investigation the northern and southern parts of the Sandur schist belt were structurally mapped in detail and the entire belt was covered by reconnaissance traverses and photogeological mapping. The schist belt has a lens-shaped geometry, about 60 km long and with a maximum width of 18 km in the central part. Two belts of metasedimentary rocks, dominated by banded iron formation (BIF), occur on the eastern and western flanks of the belt and are separated by a thick pile of metabasic rocks in the central Sandur valley (Fig. 2). There is a distinct difference in the sedimentary assemblages in the two flanks (Fig. 3). In the western belt the basal metabasalt is overlain by an impersistent quartzite–carbonate–graywacke–pelite horizon, which is followed by manganiferous phyllite with chert bands and finally by BIF. The quartzite–carbonate–graywacke association and the manganiferous horizons are absent in the eastern belt. The western contact of the schist belt is a depositional or eruptive one, the direction of younging in the sediments being consistently away from the Peninsular Gneiss. The eastern boundary is not well exposed, but it appears as a lineament in the satellite imageries and probably represents a dislocation zone along which the younger granite (2.5–2.6 Ga old, Taylor *et al.* 1988, Friend & Nutman 1991) has overridden the supracrustal rocks.

REGIONAL STRUCTURAL PATTERN

The outcrop of the eastern metasedimentary belt shows a broad eastward convexity which is absent in the western belt (Fig. 2). The bedding is generally steeply dipping and in the eastern belt the regional strike varies from 150° in the south to about 115° in the north. In the western belt a major sinistral fold pair is present near Deogiri in the southern part (Figs. 2 and 4). The average strike of bedding on the long limb is 135°, while that on the short limb is 90°. The NNW–SSE-trending ridge of BIF north of Deogiri represents a nearly isoclinal fold with a décollement at its base; it represents the antiformal fold of the sinistral fold pair mentioned above. The hinge of this fold is exposed at the northern tip of the ridge (Figs. 2 and 4). Statistical analyses of the orientation data (see the Appendix) indicate that the axis of the sinistral fold pair plunges *ca* 45° towards the north (Sectors 2 and 3 in Table 1).

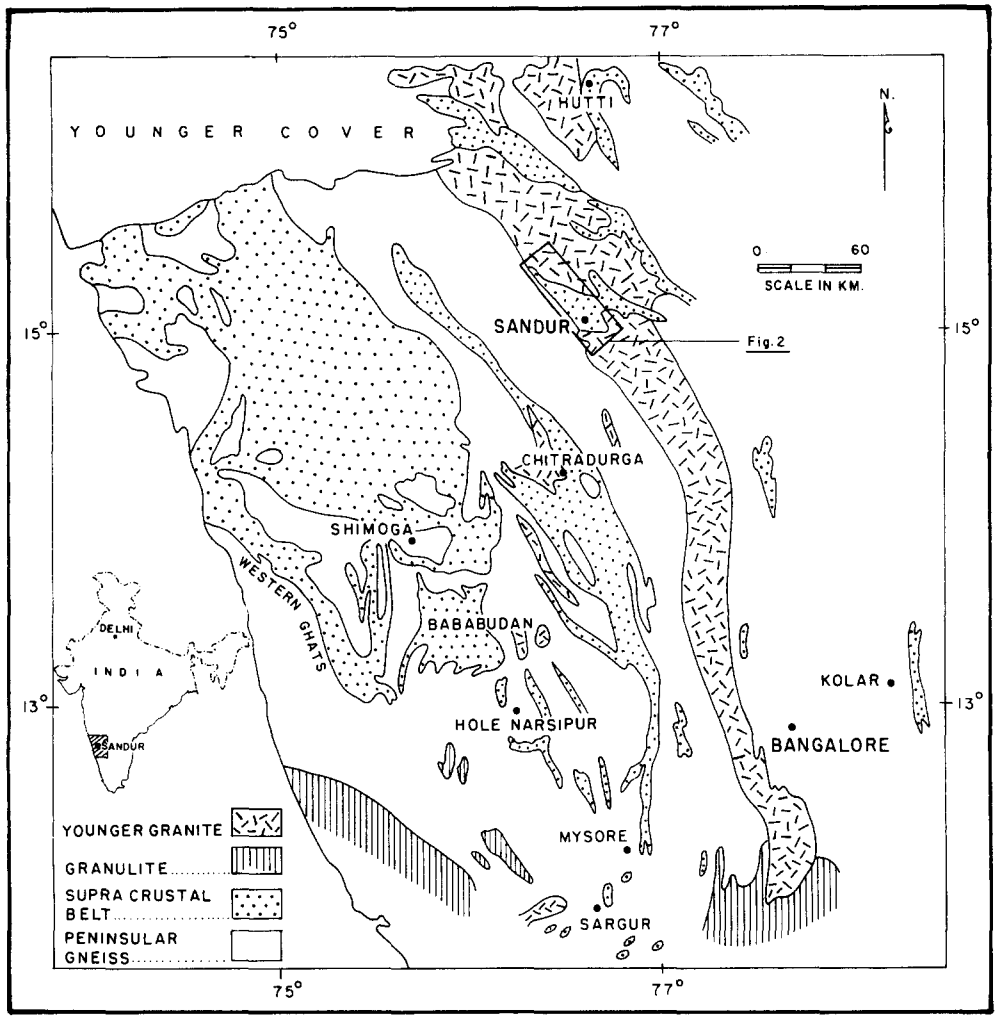

Fig. 1. Generalized geological map showing the distribution of schist belts, granites and gneisses in the Dharwar craton of South India.

The regional structure of the Sandur schist belt is traditionally interpreted to be a syncline or synclinorium (Bruce Foote 1895, Roy & Biswas 1983), which is thought to be responsible for the repetition of the metasedimentary belts on the two flanks. Our study suggests a revision of this traditional interpretation. As mentioned earlier the sedimentary assemblages in the above two belts are different and they do not represent the same stratigraphic horizon repeated by folding. Secondly, they do not join each other either at the northern or at the southern end to define any fold closure. On the contrary, the northern termination of the eastern belt near Hospet is marked by the presence of a number of isoclinal fold closures within the belt (Matin & Mukhopadhyay 1987), while the western belt continues further northward for several kilometres (Figs. 2 and 5). In the southern tip also the two belts do not join each other (Fig. 4) and here the termination of the belts is marked by tectonic interleaving of granite and supracrustal rocks (Fig. 4, inset). The granite here has developed a protomylonitic to mylonitic fabric. Thirdly, there is no systematic difference in the sense of vergence of minor folds in the eastern and western flanks, belying the existence of a regional syncline.

FOLD GEOMETRY

In the polyphasal deformation events affecting the rocks, the earliest episode (D_1) produced nearly isoclinal folds within the BIF on both major and minor scales. Closures of several large-scale D_1 isoclinal folds are traced out by the banded ferruginous quartzite (BFQ) bands in the eastern belt north of Donimalai (Figs. 2 and 4). In the Hospet region isoclinal minor folds (Fig. 6a) are prolific in the eastern band and mappable fold closures are present at the northern termination of the belt as well as within the belt. In the western belt a large isoclinal dextral fold pair (folds of Z symmetry) with long drawn-out hinges is traced out by a BFQ band (Figs. 2 and 5). The axial planes of D_1 major and minor folds are parallel to the regional attitude of bedding.

D_1 minor folds are usually isoclinal, long limbed, with high amplitude (Figs. 6a). Occasionally they are of intrafolial or disharmonic nature (Figs. 9a & b). Small tensional cracks filled up by quartz veins occur in some minor folds. The majority of such veins are oriented at high angles to the axial trace (Fig. 10), indicating extension parallel to the axial trace. Some veins show sigmoidal form as a result of their growth and rotation

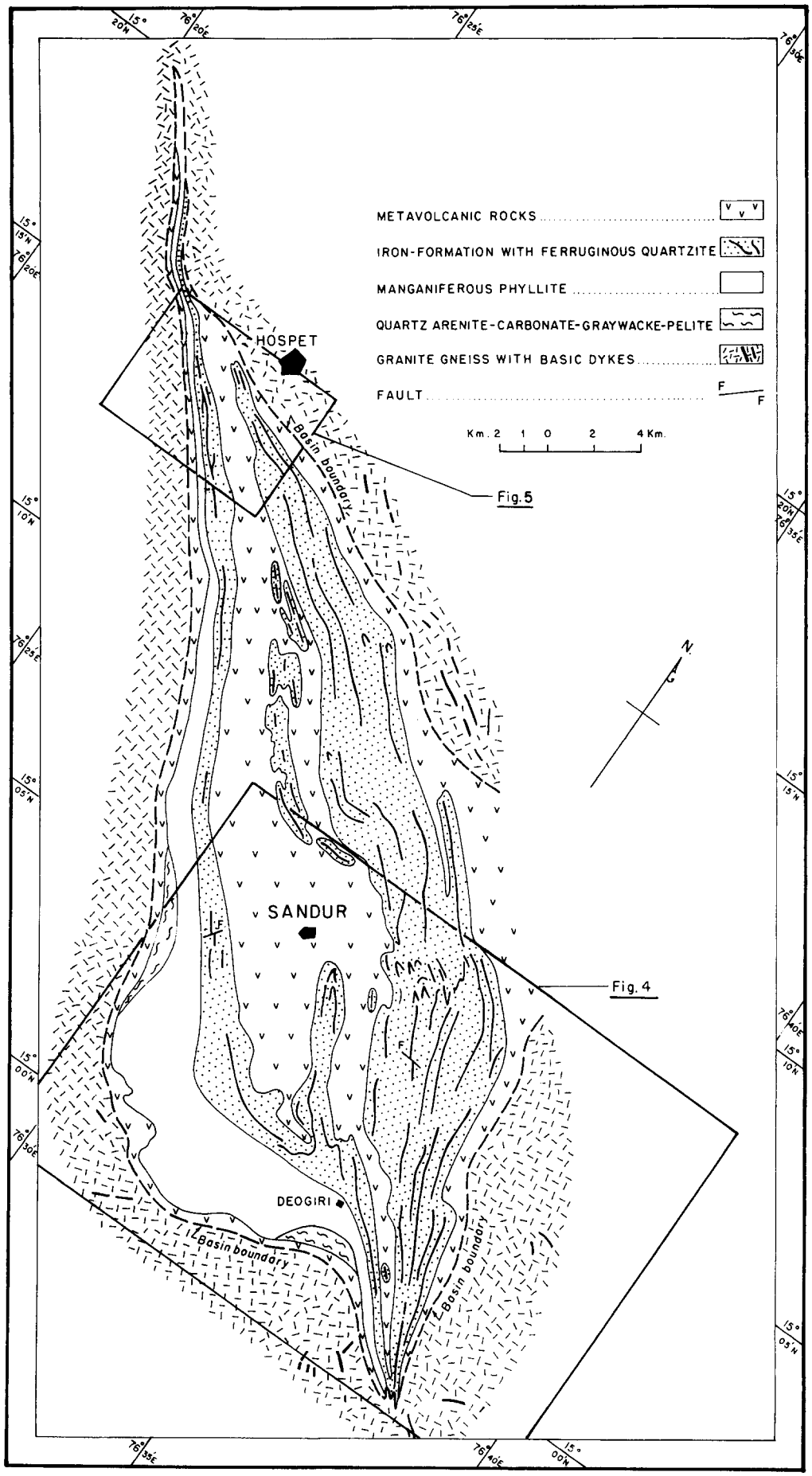

Fig. 2. Geological map of the Sandur schist belt, based on photogeological study and detailed mapping in the northern and southern parts.

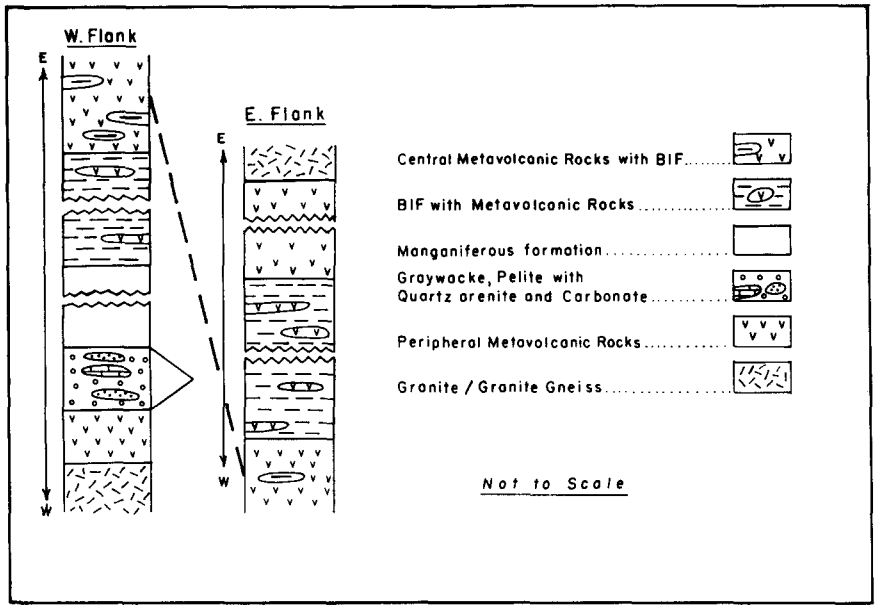

Fig. 3. Generalized stratigraphic columns in the western and eastern flanks of the Sandur schist belt.

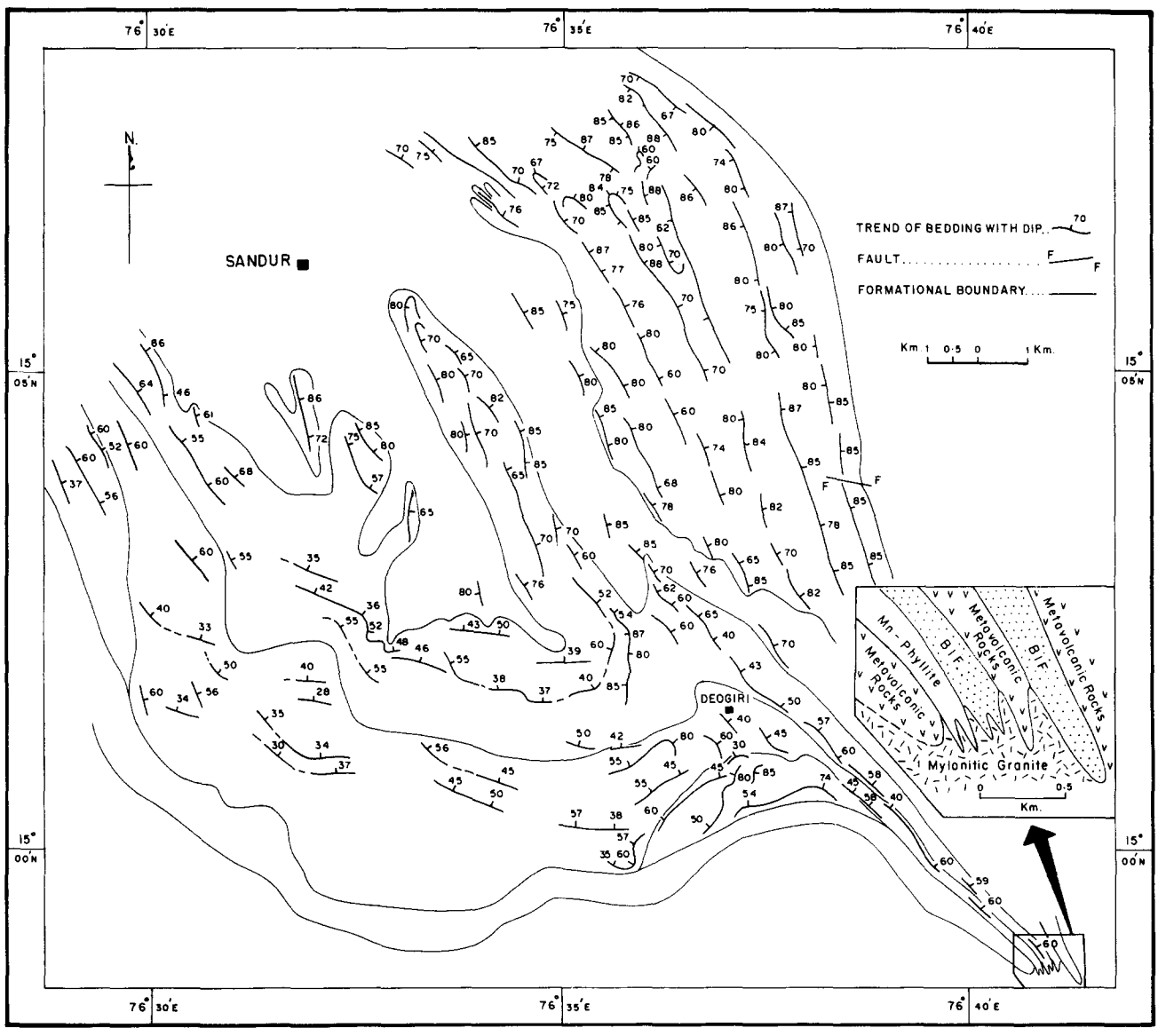

Fig. 4. Trend map of bedding in the Deogiri–Donimalai area, southern part of the Sandur schist belt.

Table 1. Orientation data for structural elements in different sectors of the Sandur schist belt

Sector number	Structural element	Plunge of lineation or pole to plane maximum (corresponding to V_1) amount (°)	direction (°)	Plunge of pole to best-fit plane (corresponding to V_3) amount (°)	direction (°)
1	S_0	03	242	—	—
(Donimalai)	S_1/S_2	13	251	67	014
	AP_1	01	063	—	—
	AP_2	03	271	—	—
	Fa_1	84	171	—	—
	Fa_2	75	019	07	262
2	S_0	35	226	46	004
(Deogiri south)	S_1/S_2	20	253	—	—
	AP_1	27	242	—	—
	AP_2	29	250	—	—
	Fa_1	42	349	26	233
	Fa_2	—	—	07	258
3	S_0	48	182	42	356
(Deogiri)	AP_2	08	071	—	—
	Fa_2	41	337	—	—
4	S_0	46	229	—	—
(Yeshwantnagar)	S_1/S_2	14	250	—	—
	AP_2	07	077	—	—
	Fa_2	34	352	—	—
5	S_0	21	245	68	069
(Deogiri north)	S_1/S_2	07	250	—	—
6	S_0	16	027	—	—
(Hospet east)	S_1	22	034	—	—
	AP_1	17	025	—	—
	AP_2	19	049	—	—
	Fa_1	70	196	—	—
	Fa_2	71	261	17	050
7	S_0	09	053	—	—
(Hospet west)	S_1	08	047	—	—
	AP_1	13	053	—	—
	AP_2	18	075	—	—
	Fa_1	—	—	12	061
	Fa_2	65	184	13	064

S_0—bedding; S_1—D_1 schistosity; S_1/S_2—undifferentiated D_1 schistosity and D_2 crenulation cleavage; AP_1—D_1 axial plane; AP_2—D_2 axial plane; Fa_1—D_1 fold axis and lineation; Fa_2—D_2 fold axis and lineation.

during progressive deformation related to layer-parallel slip (Ramsay & Huber 1987, p. 452). On fold limbs the vein geometry shows a wide range of variation because here the maximum complexity of incremental strain sequence occurs. Radial tensional veins caused by tangential longitudinal strain are formed in the outermost arcs (Fig. 10).

D_1 schistosity, developed within the pelitic schist, metagraywacke and metatuff, is of anastomosing, rough or smooth type (Powell 1979). Elongation of quartz clasts, development of 'whiskers' of chlorite against such clasts (Fig. 7a), and solution seams (Fig. 7c) parallel to the schistosity are commonly observed features. 'Refraction' (Fig. 7b) is observed in banded pelite. In some fine-grained argillitic rocks there is a bedding-parallel planar fabric which was formed during sedimentation or diagenesis and was probably accentuated by mimetic recrystallization. In such rocks the D_1 axial plane fabric is of the nature of crenulation cleavage (Fig. 7c) (cf. Borradaile *et al.* 1982). Closely spaced fractures, often filled with ferruginous material, are parallel to the axial planes of D_1 folds in quartzose layers of BFQ. They show convergent fanning in the hinge region.

The isoclinal D_1 folds with axial planes parallel to the regional attitude of bedding are indicative of strong flattening normal to the trend of the schist belt at this stage of deformation.

The second episode of deformation (D_2) produced aysmmetric folds with consistent sinistral sense of vergence (Fig. 6b) throughout the schist belt. The major sinistral fold pair near Deogiri (Figs. 2 and 4) belongs to this episode.

D_1 folds are seen to be refolded by D_2 folds (Figs. 6d and 9h & i). Occasionally quartz veins parallel to the D_2 axial planes cut across the D_1 folds (Fig. 6c). Although the D_1 and D_2 minor folds are prolific within the BFQ, examples of refolded folds are rather rare. Often the later folds are confined to only one limb of earlier folds and occur as incongruous minor folds. This is due to the mechanical difficulty of buckling of non-parallel planes (Ramsay 1967, pp. 546–548). Ramsay has discussed that buckling of non-parallel planes may lead to sliding along

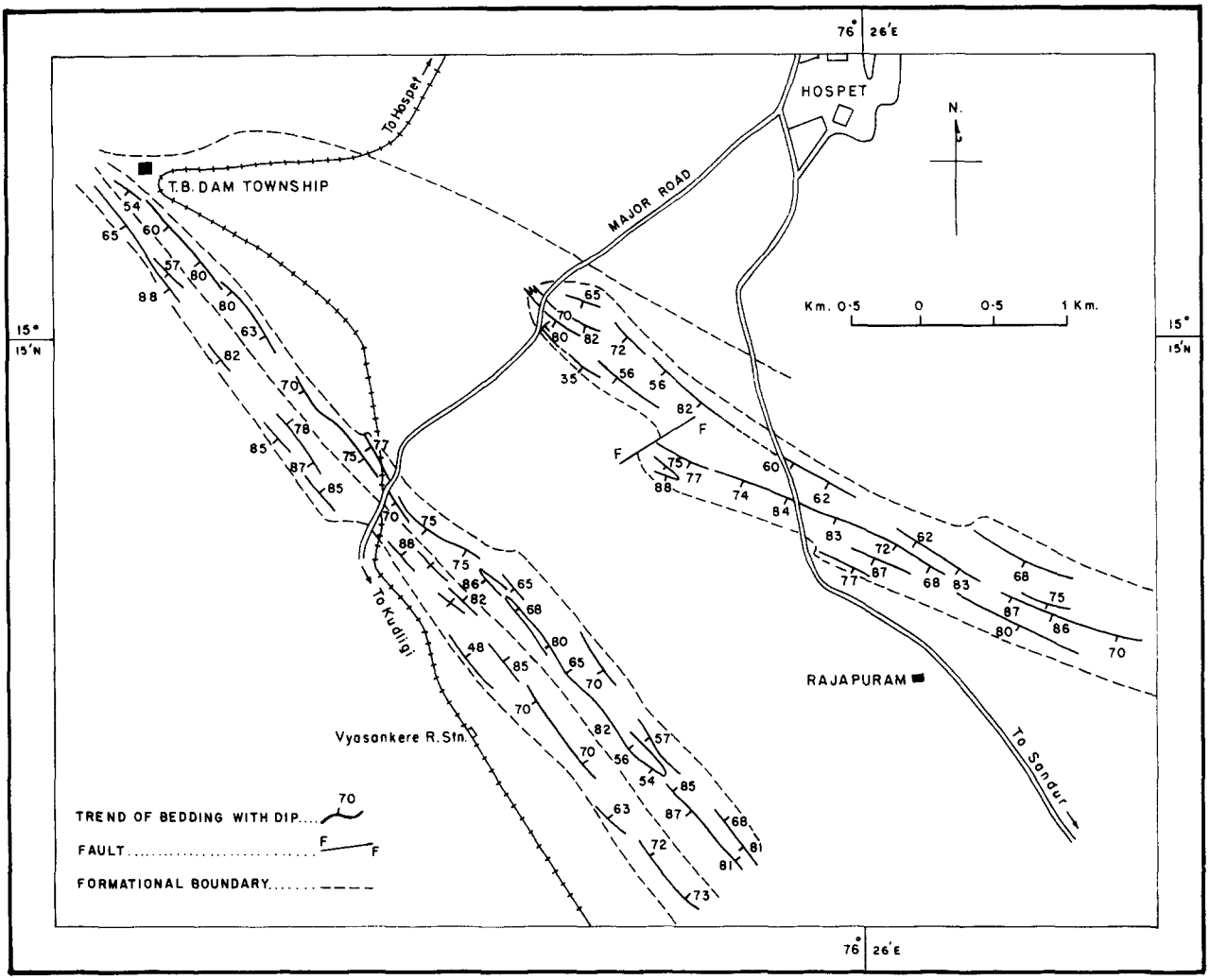

Fig. 5. Trend map of bedding in the Hospet area, northern part of the Sandur schist belt.

early axial surfaces or complicated strain patterns may be set up; these are avoided if the later folds are confined within domains where the bedding retains a planar attitude (Mukhopadhyay & Baral 1985).

D_2 folds in BFQ are commonly disharmonic, of intrafolial nature, strongly asymmetric, and bounded on either side by planar bedding surfaces (Figs. 9f & g). Such folds presumably owe their origin to layer-parallel simple shear. In some asymmetric folds the long limbs are attenuated while the short limbs are either thickened or microfolded thereby attesting that the bisecting surface between the limbs does not coincide with the XY plane (where $X \geq Y \geq Z$ represent the principal directions and magnitudes of strain). High-amplitude folds often have décollement surfaces at their base separating them from unfolded strata. Such disharmonic geometry with décollement is spectacularly displayed on a large scale in the western BIF band on the ridge extending from Deogiri (Figs. 2 and 4). An argillaceous band at the base of this isoclinal fold facilitated detachment along this horizon.

Curved fold hinges, convergence and divergence of hinges of neighbouring folds, branching, coalescence and en échelon distribution of hinges are very common. Sheath folds with subparallel hinge lines are occasionally seen (Fig. 8a). These are interpreted to have developed as a result of strong compression and/or layer-parallel shear on D_1 folds having slight initial curvature of the axes. If individual early folds had slightly curved axes, strong simple shear with movement direction at high angle to the early axes would amplify the curvature and give rise to sheath folds (Cobbold & Quinquis 1980). The axial traces of the sheath folds are locally bent by D_2 folds giving rise to bent 'eyes' showing crescent shaped outcrop patterns (Fig. 8b). Plunge 'inversion' along individual axial traces showing the same sense of closure has caused change over of some minor antiforms through neutral folds to synforms (cf. fig. 10-27 in Ramsay 1967). A related phenomenon is the variable orientation of lineations on successive planar bedding surfaces (Fig. 8d). All the variability in the orientation of fold axes described above is interpreted to be due to progressive development of folds and rotation of their axes in non-coaxial deformation (simple shear) during the D_2 episode.

The presence of a strong component of sinistral layer-parallel shear during D_2 deformation is indicated by the intrafolial nature and consistent sense of asymmetry of the folds, and their development in zones bounded by planar bedding on either side (Figs. 6b and 9f & g).

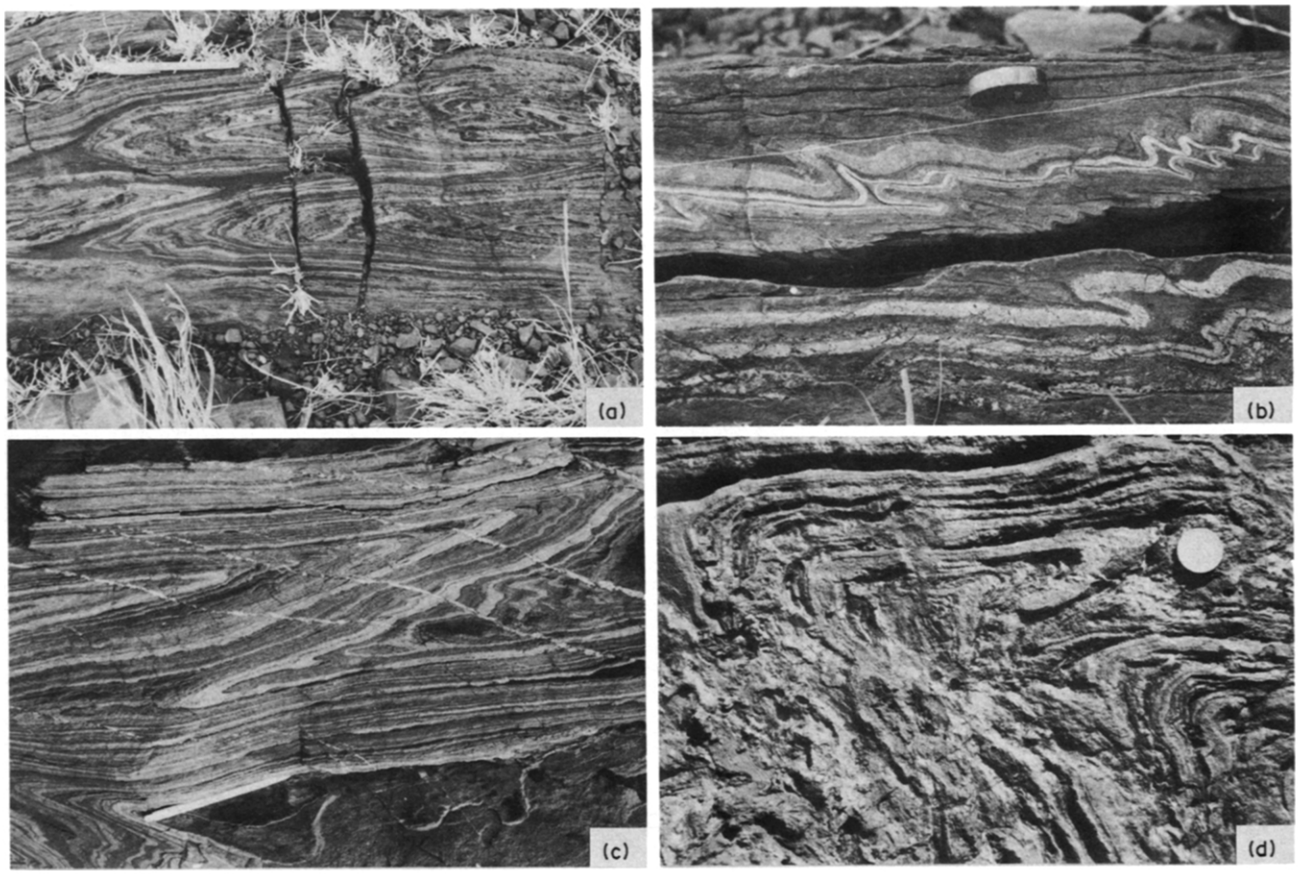

Fig. 6. (a) D_1 isoclinal folds. (b) D_2 sinistral folds. (c) D_1 isoclinal folds cut across by quartz veins parallel to D_2 axial planes. (d) Refolding of D_1 fold by D_2.

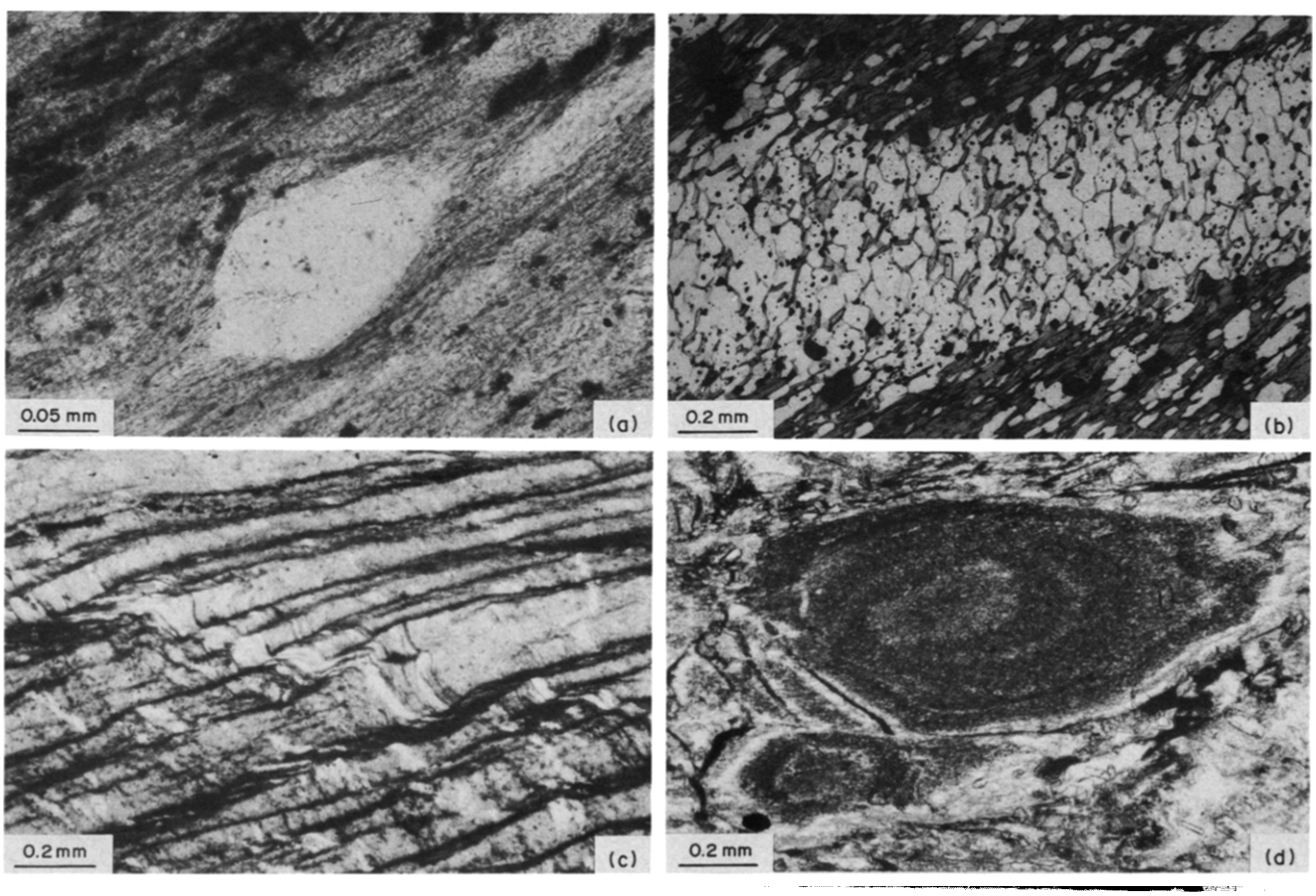

Fig. 7. (a) Elongated quartz clasts with 'whiskers' of chlorite at the ends. (b) 'Refraction' of D_1 schistosity in banded pelite. (c) D_1 crenulation cleavage in pelite. (d) Accretionary lapillae in tuff.

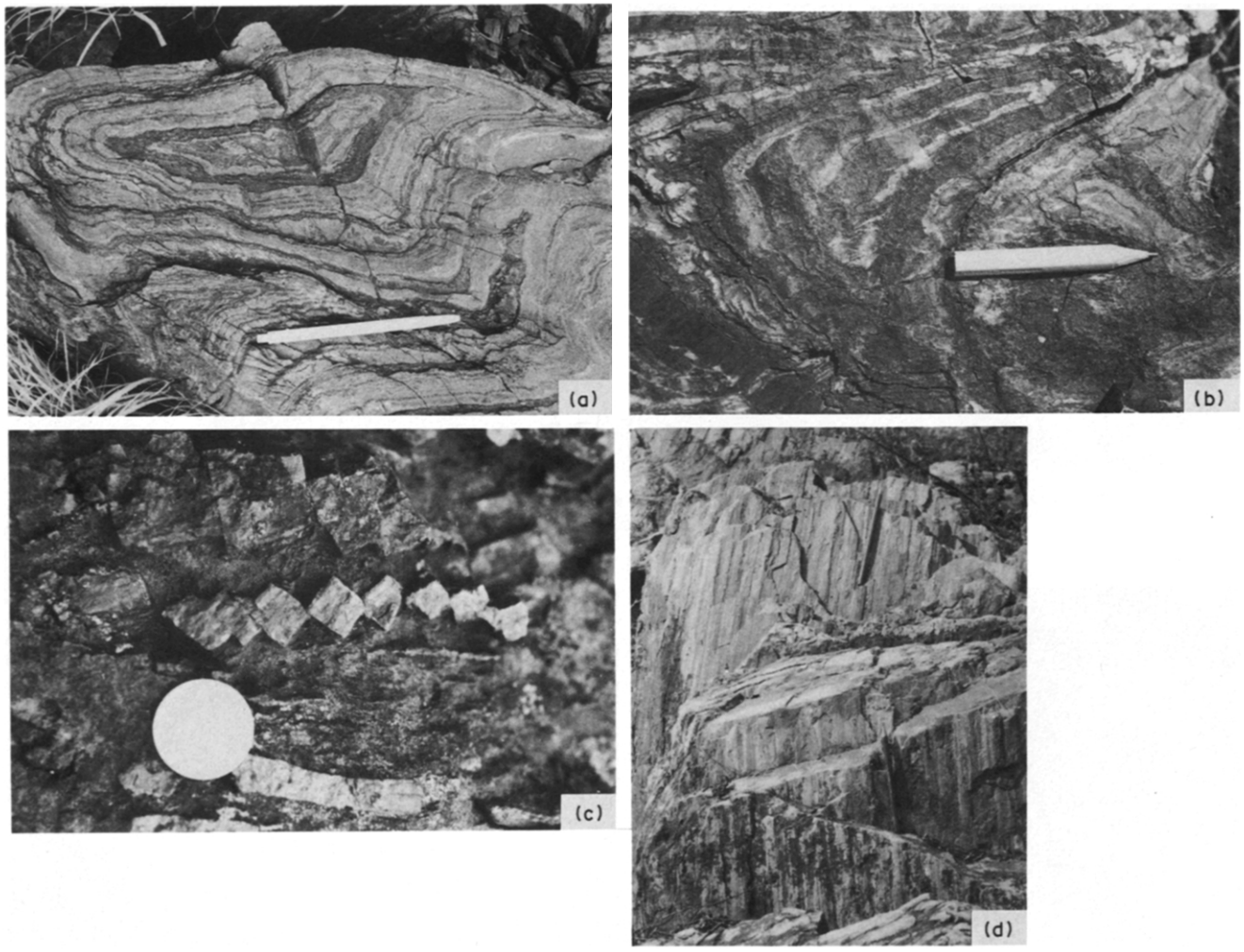

Fig. 8. (a) D_1 sheath fold. The sinistral fold with oblique axial plane is D_2. (b) D_1 sheath fold bent by D_2 fold. (c) Book-shelf sliding in transversely fractured chert band in BIF. (d) Non-parallel D_1 lineation on successive parallel bedding surfaces.

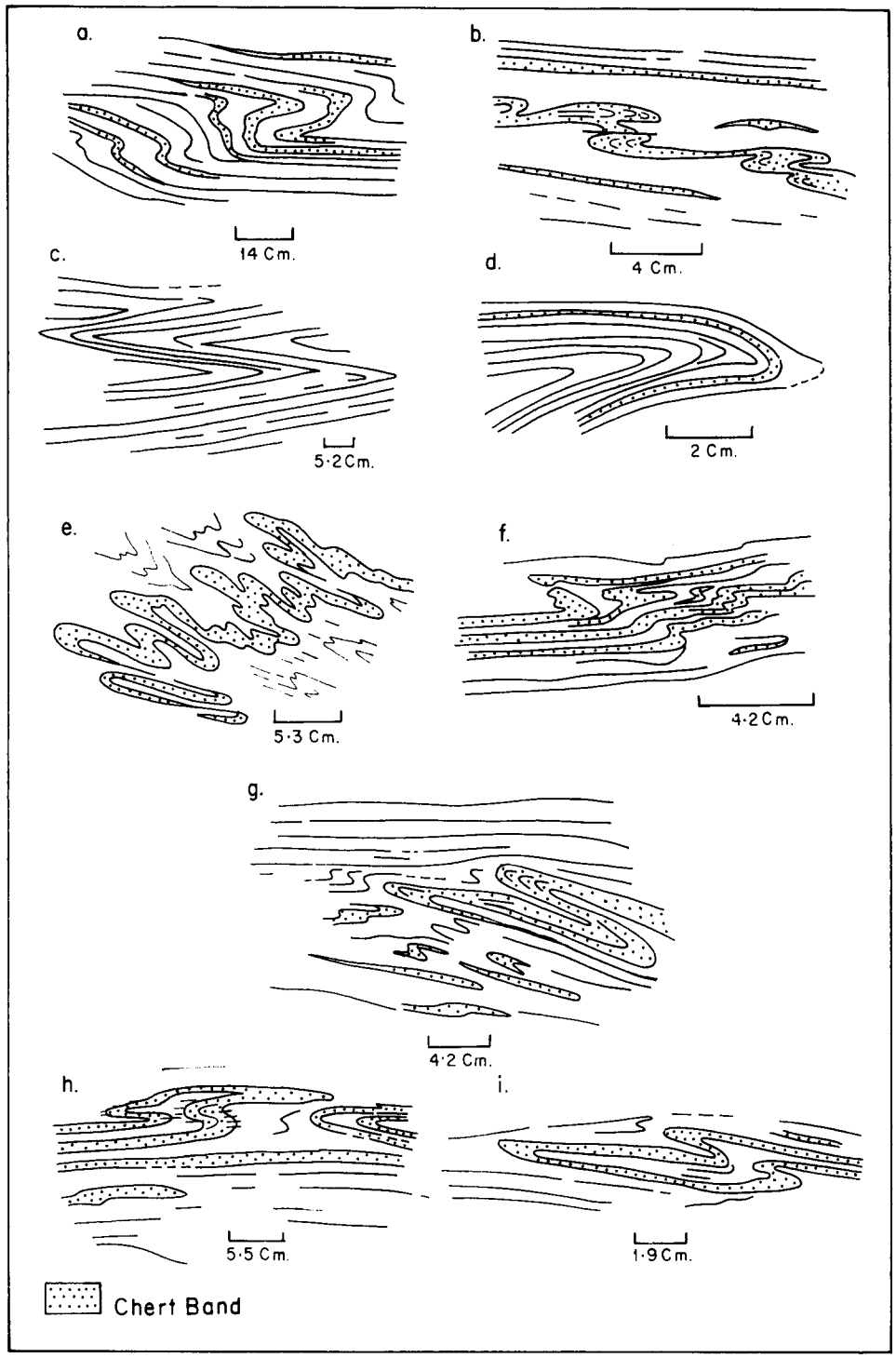

Fig. 9. (a) Dextral disharmonic D_1 fold. (b) Dextral D_1 intrafolial folds. (c) D_1 chevron folds. (d) D_1 fold, class 1B geometry with rounded hinge in thin chert band; class 3 geometry with angular hinge in iron oxide layer. (e)–(g) Sinistral disharmonic D_2 folds. (h) & (i) D_1 isocline refolded by D_2 sinistral fold.

Other indicators of simple shear are the local presence of sheath folds (Fig. 8a), book-shelf sliding in transversely fractured chert bands (Fig. 8c), and occurrence of *S–C* fabric within lenticular domains in schist and presence of narrow ductile shear zones in metabasic rocks. The orientation of the stretching lineation and of the axes of the sheath folds indicates a steep plunge of the stretching direction during D_2 deformation.

The stretching lineation observed in the schistose rocks is steeply plunging and the D_1 and D_2 fold axes are clustered around this direction. During the D_1 deformation the maximum compression was nearly perpendicular to the fold axial planes while during D_2, the shortening being oblique to the layer-parallel anisotropy, the deformation took the nature of transpression with two simultaneously acting components. The dominant component was shortening at a high angle to the strike of S_0/S_1 causing a thrust type movement and the formation of a steeply plunging stretching lineation. The other component was a consistent sinistral strike-slip.

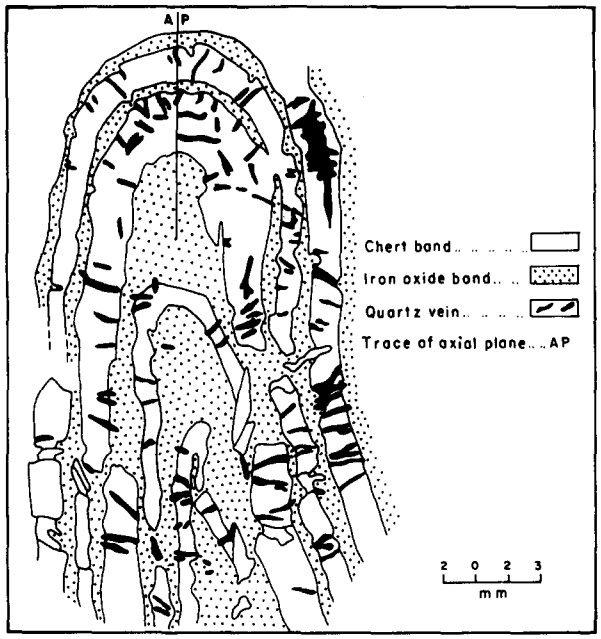

Fig. 10. Tensional veins in chert bands in a D_1 fold. Note the very rounded hinge of the nearly isoclinal fold.

The interplay of these two led to the rotation of all fold axes towards the stretching direction and development of sinistral asymmetry of the folds.

Except for the asymmetry, there is not much difference in the style of D_1 and D_2 minor folds. Both are tight to isoclinal with high amplitude to wavelength ratio. The relative competency of the different bands in BIF is evident from the differences in fold geometry of adjacent layers. The chert–quartzite bands invariably behaved as more competent ones in comparison to the ferruginous layers and show class 1B or class 1C geometry, while the iron oxide layers usually show class 3 geometry. Z/Y values for the profile planes computed from thickness measurements in the chert bands (Ramsay 1967, pp. 412–413, Hudleston 1973) range from 0.1 to 0.8. The chert bands embedded in thick iron oxide matrix often show broad rounded hinges with forms approaching elastica curves (Figs. 9d & e and 10), suggesting a high competency contrast. In multilayered units where the thickness ratios of competent to incompetent layers is high the folds have angular hinges (Fig. 9c) (cf. Ramsay & Huber 1987, Model E, fig. 20-11). Sometimes a multilayer composed of several siliceous and iron oxide bands behaves as a competent unit showing class 1C geometry and is separated from another competent unit by a thick iron oxide layer showing class 3 geometry.

The similarity in style and the closeness in orientation of the axes and axial planes of D_1 and D_2 folds suggest that these two sets of structures are not products of entirely unrelated episodes of deformation, but were probably formed during the early and late stages of a progressive deformation history.

A noteworthy feature in the structural pattern is that the deformation is mostly concentrated within the two metasedimentary belts and the overall strain is low in the central metavolcanic unit except in narrow shear zones. The X/Y and Y/Z values calculated from deformed accretionary lapillae from one locality (Fig. 7d) within the central metavolcanic unit are, respectively, 1.6 and 1.7. This is much less than the strain values suggested by the long-limbed flattened isoclinal folds within the BIF. Concentration of layer-parallel shear within the metasedimentary unit is probably responsible for this strain heterogeneity.

The regional structural pattern in the area is controlled by the D_1 and D_2 episodes. However, there are two other minor episodes of deformation. Weak longitudinal compression during D_3 deformation gave rise to folds and gentle warps on bedding and kinks on schistosity which have transverse axial planes. These are sometimes polyclinal or box-like in nature. The broad curvature of bedding strike in the eastern BIF belt is also a result of the D_3 deformation. D_4 structures are only local and consist of minor folds with subhorizontal axial planes.

ORIENTATION PATTERN

For structural analysis the area mapped in detail has been subdivided into seven sectors, five in the Donimalai–Deogiri region, and two in the Hospet region (Fig. 11). The regional orientation pattern of different planar and linear structural elements has been statistically analysed by computing the eigenvalues and eigenvectors of the orientation matrices for different structural elements in each sector (Woodcock 1977, Davis 1986, pp. 334–339). The details are given in the Appendix and the results are summarized in Table 1. A few representative equal-area projection diagrams are given in Fig. 11.

The strike of S_1 and of D_1 axial planes is subparallel to S_0, while that of the D_2 axial planes makes a small angle with S_0, which is consistent with the sinistral sense of vergence of D_2 folds. D_1 and D_2 fold axes have variable plunges, but are in general moderately to steeply plunging. The data show a greater variability in the orientation of the fold axes than of the axial planes (Table 1). In many of the sectors the axial planes show point maxima, while the axes show a great circle distribution which is either uniform or with point maxima. The great circle invariably coincides with the corresponding modal axial plane (Table 1, Fig. 11). The above geometrical pattern is ascribed to progressive rotation of fold axes towards the stretching direction during D_2 simple shear deformation. Once folds are nucleated in simple shear due to local perturbation, their axial planes would rotate towards the movement plane, and their axes would rotate towards the stretching direction. Since the axes might have initially formed at various angles to the movement direction (Bell & Hammond 1984), they would rotate by different amounts. Hence, progressive simple shear would ultimately give rise to an orientation pattern in which the fold axes would be distributed on the mean axial plane. Whether they would show a cluster on the axial plane or would be widely dispersed

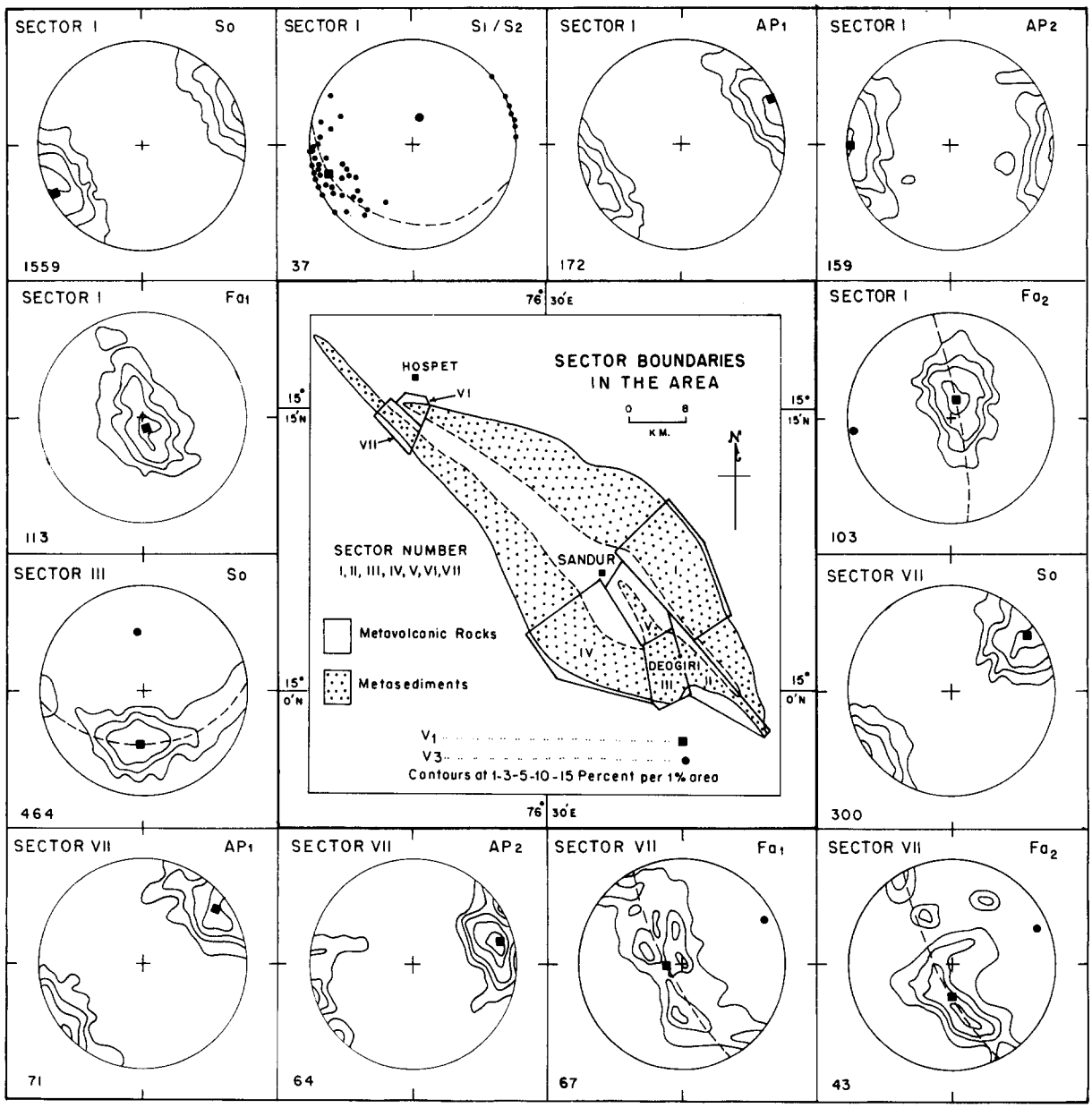

Fig. 11. Selected equal-area plots of structural elements from different sectors.

would depend on the initial variability of the axes and the amount of rotation suffered by them, which in turn would be controlled by the intensity of deformation and the time of development of the fold during the progressive deformation history.

DEFORMATION AND METAMORPHISM

The overall grade of metamorphism is low. The quartz grains in the BFQ are micropolygonal in shape and the size generally varies from 0.03 to 0.045 mm. In the more recrystallized parts the grain size reaches as much as 1 mm. Grain size of quartz in BFQ has been suggested to be an indicator of the grade of metamorphism (James 1955, Gross 1961, Dorr 1964, Klein 1973), and the measured sizes in the present area indicate chlorite to biotite zone conditions. Porphyroblasts of higher grade minerals like andalusite, garnet and staurolite are sporadically recorded in the mica schists, mostly near the basin margin (cf. Roy & Biswas 1979).

Parallelism of chlorite and biotite with D_1 schistosity indicates that their recrystallization was synkinematic with D_1 deformation. D_2 deformation was accompanied by occasional and incipient growth of mica flakes parallel to the crenulation cleavage. The nature of inclusion trails indicate that andalusite, garnet and staurolite are predominantly post-tectonic with respect to D_1 deformation (Roy & Biswas 1979). The relation of andalusite porphyroblasts to D_2 crenulation cleavage is variable. In some instances andalusite appears to be earlier and the crenulation cleavage swerves round the porphyroblasts which contain straight inclusion trails while the external schistosity is puckered. In other instances the andalusite has grown after the development of crenulation cleavage and slivers of andalusite have grown along the mica-rich

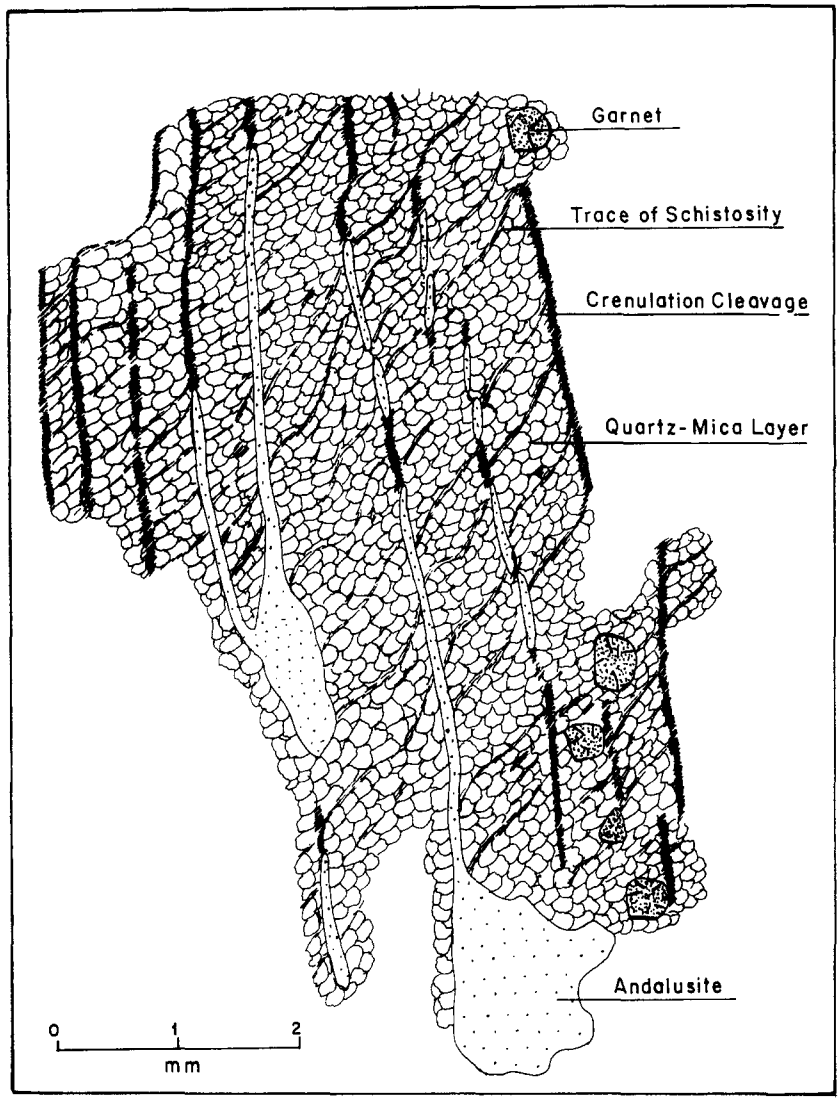

Fig. 12. Sketch from a photomicrograph showing slivers of andalusite growing along the mica-rich domains in differentiated D_2 crenulation cleavage.

domains of the cleavage (Fig. 12). Where the andalusite porphyroblasts have grown across the quartz-rich and mica-rich cleavage domains, the boundaries between these domains continue within the porphyroblasts as boundaries between inclusion-free and inclusion-rich zones. Therefore, while the growth of garnet and staurolite stopped before the D_2 deformation, andalusite continued to grow even after D_2.

CONCLUSIONS

The geometry of structures indicates that both flattening and simple shear played major roles in the deformation history of the Sandur schist belt. Compression probably dominated in the early stages and simple shear in the later stages. The tectonic regime may be compared to one of transpression (cf. Chadwick *et al.* 1989). The presence of a significant left-lateral strike-slip component is evident from the sinistral sense of vergence of D_2 folds. The deformation, particularly the simple shear, was concentrated within the layered sediments, which explains the difference in the intensity of strain within the metavolcanics and within the BIF. The variability in orientation of fold axes was caused by their formation at different stages of deformation and the progressive rotation of their axes towards the stretching direction during D_2 simple shear. The grade of metamorphism remained low during D_1 deformation. The thermal peak represented by the crystallization of minerals like andalusite, garnet and staurolite was attained prior to or during the D_2 deformation.

Acknowledgements—Financial assistance was received by one of us (A. Matin) from the University Grants Commission for the work. We are grateful to the National Mineral Development Corporation, the Sandur Manganese and Iron Ores Limited and to Dr P. S. N. Murthy for their co-operation during the field work. Two anonymous reviewers contributed useful comments and criticisms.

REFERENCES

Bell, T. H. & Hammond, R. L. 1984. On the internal geometry of mylonite zones. *J. Geol.* **92**, 667–686.

Borradaile, G. J., Bayly, M. B. & Powell, C. McA. 1982. *Atlas of*

Deformational and Metamorphic Rock Fabrics. Springer, New York.
Bruce Foote, B. 1895. The geology of Bellary district, Madras Presidency. *Mem. geol. Surv. India* **25,** 1–218.
Chadwick, B., Ramakrishnan, M. and Viswanatha, M. N. 1989. Facies distribution and structure of a Dharwar volcanosedimentary basin: evidence for late Archaean transpression in southern India? *J. geol. Soc. Lond.* **146,** 825–834.
Cobbold, P. R. & Quinquis, H. 1980. Development of sheath folds in shear regimes. *J. Struct. Geol.* **2,** 119–126.
Davis, J. C. 1986. *Statistics and Data Analysis in Geology* (2nd edn). John Wiley, New York.
Dorr, J. V. N. 1964. Supergene ores of Minas Gerais, Brazil. *Econ. Geol.* **59,** 1203–1240.
Friend, C. R. L. & Nutman, A. P. 1991. SHRIMP U–Pb geochronology of the Closepet Granite and Peninsular Gneiss, Karnataka, South India. *J. geol. Soc. India* **38,** 357–368.
Gross, G. A. 1961. Metamorphism of iron-formations and its bearing on their beneficiation. *Bull. Can. Mineral. Metall.* **54,** 30–37.
Hudleston, P. J. 1973. Fold morphology and some geometrical implications of theories of fold development. *Tectonophysics* **16,** 1–46.
James. H. L. 1955. Zones of regional metamorphism in the Precambrian of northern Michigan. *Bull. geol. Soc. Am.* **66,** 1455–1487.
Klein, C. 1973. Changes in mineral assemblages with metamorphism of some banded Precambrian iron-formations. *Econ. Geol.* **58,** 1075–1088.
Matin, A. & Mukhopadhyay, D. 1987. Structural interpretation of the north-western termination of the Sandur schist belt. *Indian J. Earth Sci.* **14,** 214–216.
Mukhopadhyay, D. & Baral, M. C. 1985. Structural geometry of Dharwar rocks near Chitradurga. *J. geol. Soc. India* **26,** 547–566.
Powell, C. McA. 1979. A morphological classification of rock cleavage. *Tectonophysics* **58,** 21–34.
Ramsay, J. G. 1967. *Folding and Fracturing of Rocks*. McGraw-Hill, New York.
Ramsay, J. G. & Huber, M. I. 1987. *The Techniques of Modern Structural Geology, Volume* 2: *Folds and Fractures*. Academic Press, London.
Roy, A. & Biswas, S. K. 1979. Metamorphic history of the Sandur schist belt, Karnataka. *J. geol. Soc. India* **20,** 179–187.
Roy, A. & Biswas, S. K. 1983. Stratigraphy and structure of the Sandur schist belt, Karnataka. *J. geol. Soc. India* **24,** 19–29.
Swaminath, J., Ramakrishnan, M. & Viswanatha, M. N. 1976. Dharwar stratigraphic model and Karnataka cratonic evolution. *Rec. geol. Surv. India* **107,** 149–175.
Taylor, P. N., Chadwick, B., Friend, C. R. L., Ramakrishnan, M., Moorbath, S. & Viswanatha, M. N. 1988. New age data on the geological evolution of southern India. *J. geol. Soc. India* **31,** 155–157.
Woodcock, N. H. 1977. Specification of fabric shapes using an eigenvalue method. *Bull. geol. Soc. Am.* **88,** 1231–1236.

APPENDIX

The orientation of any line in space (either a linear element or the pole to a planar element) is specified by its direction cosines l, m, n with respect to three reference axes that point horizontally north, horizontally east and vertically down. The orientation matrix is then given as below:

$$M = \begin{vmatrix} \Sigma l^2 & \Sigma lm & \Sigma ln \\ \Sigma ml & \Sigma m^2 & \Sigma mn \\ \Sigma nl & \Sigma nm & \Sigma n^2 \end{vmatrix}.$$

The three eigenvalues of this matrix are labelled as λ_1, λ_2 and λ_3 in order of increasing magnitude (Woodcock 1977, Davis 1986). It is customary to use the normalized values $\bar{\lambda} = \lambda_i/N$, where N is the total number of measurements. Associated with these eigenvalues are the three eigenvectors V_1, V_2 and V_3. V_1 corresponds to the highest density of points in the projection diagram and V_3 is the pole to the best-fit great circle.

Woodcock (1977) proposed that the distribution pattern may be depicted by plotting logs of the ratios of normalized eigenvalues on

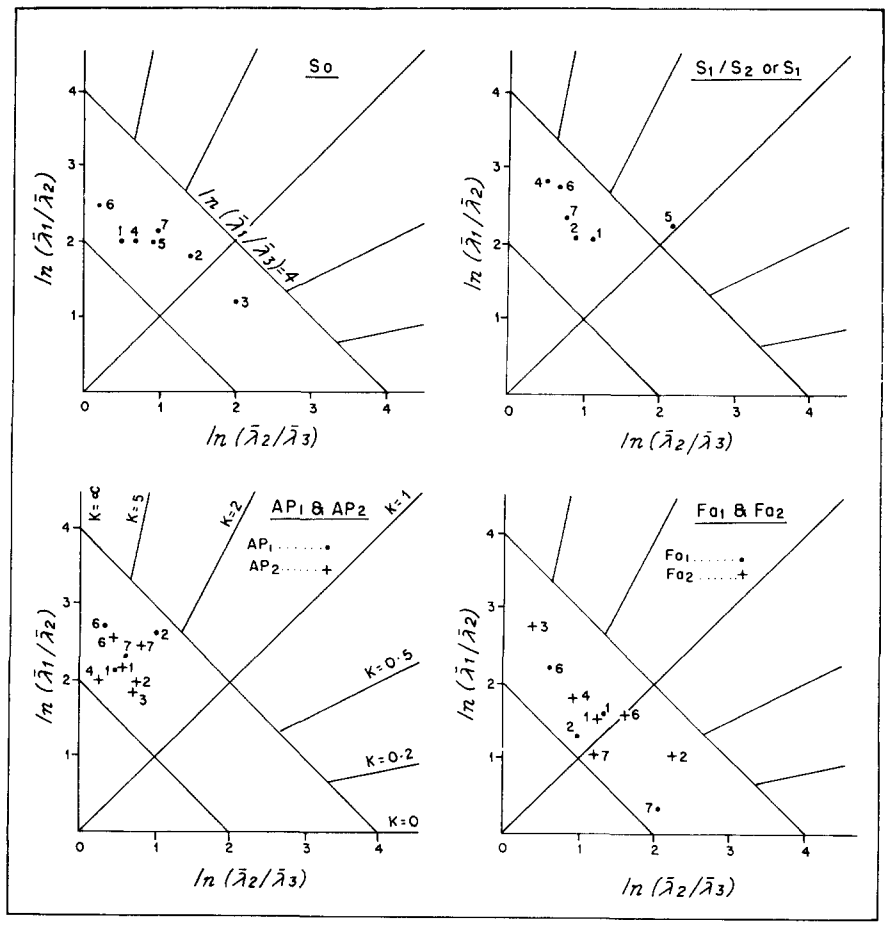

Fig. A1. Plots of ratios of normalized eigenvalues for structural elements in the different sectors (cf. Woodcock 1977).

orthogonal co-ordinates axes, ln (λ_2/λ_3) vs ln (λ_1/λ_2). The parameter $k = \ln(\lambda_1/\lambda_2)/\ln(\lambda_2/\lambda_3)$ is an indicator of the distribution pattern, Distributions that have equal girdle and cluster tendencies plot along the line $k = 1$. Those with dominant girdle tendencies $(0 \leq k < 1)$ plot below the line, and clusters $(1 < k \leq \infty)$ plot above the line. In this study the distribution pattern is characterized as a point maximum if the value of k is >2; if k is >0.5 but <2 the distribution is a girdle along with a point maximum; and if k is <0.5 the distribution is nearly uniform on a girdle.

The orientations of the eigenvectors V_1 and V_3 for the structural elements in different sectors are given in Table 1 and the plots of ratios of normalized eigenvalues are given in Fig. A1. When the measurements for a particular structural element are too few (<20) they are not included in Table 1 or in the plots (Fig. A1). The geometry of D_1 and D_2 structures only are discussed, as the D_3 and D_4 structures are locally developed and do not affect the regional structural pattern. In some sectors S_1 and S_2 could not be unambiguously distinguished in the field; hence these are plotted together as S_1/S_2.